

UNCLASSIFIED

AD 403 877

*Reproduced
by the*

DEFENSE DOCUMENTATION CENTER

FOR

SCIENTIFIC AND TECHNICAL INFORMATION

CAMERON STATION, ALEXANDRIA, VIRGINIA



UNCLASSIFIED

NOTICE: When government or other drawings, specifications or other data are used for any purpose other than in connection with a definitely related government procurement operation, the U. S. Government thereby incurs no responsibility, nor any obligation whatsoever; and the fact that the Government may have formulated, furnished, or in any way supplied the said drawings, specifications, or other data is not to be regarded by implication or otherwise as in any manner licensing the holder or any other person or corporation, or conveying any rights or permission to manufacture, use or sell any patented invention that may in any way be related thereto.

63-3-4

①

Technical Report No. 7

Monr 839(12)

NR 032 - 414

AD No. 4038 77

WHILE COPY

THE ANOMALOUS SCATTERING OF X-RAYS
BY BORON PHOSPHIDE AND ZINC SULFIDE

by

Z. Barnea and B. Post

Polytechnic Institute of Brooklyn
333 Jay Street, Brooklyn 1, N. Y.

Reproduction, in whole or in part, is permitted for any
purpose by the United States Government.

403 877

March 1963

76.60

MAY 17 1963

TISIA A

14 TR7

4 \$ 6.60
5 710 200

Technical Report No. 7

15
Nonr 839(12)

13
Proj. NR 032 - 414
7-11-63

6 THE ANOMALOUS SCATTERING OF X-RAYS
BY BORON PHOSPHIDE AND ZINC SULFIDE

7 NA
8 NA
9 NA

10 by
Z. Barnea and B. Post

11
12 U.
13 NA

11 mar 63
12 59 p.
13 V.F.

Polytechnic Institute of Brooklyn
333 Jay Street, Brooklyn 1, N. Y.

Reproduction, in whole or in part, is permitted for any
purpose by the United States Government.

March 1963

AN ABSTRACT

THE ANOMALOUS SCATTERING OF X RAYS

BY

BORON PHOSPHIDE AND ZINC SULFIDE

by

Zwi Barnea

Adviser: Benjamin Post

Submitted in partial fulfillment of the requirements
for the degree of Master of Science (Physics)

The dispersion of the atomic scattering factors of ^{Zn} zinc, ^S sulfur, and ^P phosphorus in selected regions of the x-ray spectrum ^{was} ~~has been~~ investigated by measuring the differences in the intensities of Bragg reflections due to the anomalous scattering of x rays by zinc sulfide and boron phosphide. Intensity differences among selected reflections occurring at identical Bragg angles, divided by the corresponding average intensities, ~~$\Delta I/I_{av}$~~ ^{were} plotted as functions of $\sin^2 \theta$ (the Bragg angle) and compared with ~~two~~ ² sets of theoretically predicted values of ~~$\Delta I/I_{av}$~~ ^{*}. The latter were obtained by applying the real and imaginary corrections calculated by Hönl (1) and Parratt and Hempstead (2) respectively, to the atomic scattering factors.

The ^S experimentally determined values of ~~$\Delta I/I_{av}$~~ ^{*} for zinc sulfide using ^{Mo} molybdenum ~~K α~~ ^{K α} radiation were ~~found to be~~ in good agreement with those from similar previous investigations ~~(3,4)~~, and appear generally to be higher than the theo-

* $\Delta I/I_{av}$ was determined

*** $\Delta I/I_{av}$ for ZnS

TABLE OF CONTENTS

	<u>Page</u>
Introduction.....	1
Dispersion.....	2
Lorentz's Dispersion Theory.....	2
Revised Lorentz Theory.....	6
The Kramers-Kallmann-Mark Theory of the Refractive Index.....	8
The Relation Between the Complex Refractive Index and the Atomic Scattering Factor.....	9
Further Developments of Dispersion Theory.....	11
The Anomalous Scattering of X Rays.....	13
Experimental Work.....	19
The Anomalous Scattering of Molybdenum $K\alpha$ Radiation by Cubic Zinc Sulfide.....	19
The Anomalous Scattering of Copper $K\alpha$ Radiation by Cubic Zinc Sulfide.....	30
Attempt to Obtain Experimental Values of the Imaginary Dispersion Corrections $\Delta f''_{Zn}$ and $\Delta f''_S$	31
The Anomalous Scattering of Chromium $K\alpha$ Radiation by Cubic Zinc Sulfide.....	39
The Anomalous Scattering of Copper and Chromium $K\alpha$ Radiation by Boron Phosphide.....	42
Attempt to Evaluate the Real and Imaginary Corrections to the Atomic Scattering Factors of Phosphorus.....	44
Discussion of Experimental Results.....	50
Appendix.....	53
Bibliography.....	56

INTRODUCTION

In recent years, as increasingly precise measurements of the intensity of Bragg diffraction peaks are becoming possible, there has been renewed interest in checking dispersion theory in the x-ray region. There is also considerable interest in dispersion, as it affects the atomic scattering factors. While it can be said that this interest is at present chiefly confined to the wavelengths in common use in x-ray diffraction investigations, where the corrections to the atomic scattering factors are important in structure-factor and similar calculations, there are indications that in the future increasing use will be made of dispersion effects at x-ray wavelengths at which they are particularly pronounced and where their use can contribute to the solution of the phase problem and to the determination of the absolute configuration of molecules (25).

DISPERSION*

The term "dispersion," first introduced to describe the behavior of light passed through a prism, was later used in referring to the reason underlying this behavior --- the variation of the index of refraction with the frequency of the incident light, --- and its meaning was finally extended to include the variation of any physical quantity with frequency.

For visible light the index of refraction of transparent media generally increases with decreasing wavelength. When the index of refraction decreases with decreasing wavelength, as is the case near absorption or emission frequencies characteristic of the substance, this effect is referred to as "anomalous dispersion."

The discovery of anomalous dispersion in the optical region (Leroux, 1862) suggested that the theory of dispersion must describe the propagation of electromagnetic radiation through a medium consisting of oscillators possessing their own natural frequencies.

LORENTZ'S DISPERSION THEORY

Lorentz was the first to propose a dispersion theory which explained the variation of the index of refraction in the region of visible light and gave the refractive indices

*The following five sections are based mainly on the discussion in "X-Rays in Theory and Experiment" by A.H. Compton and S.K. Allison, Van Nostrand Co., 1957.

for x rays in regions not too close to the critical absorption limits.

Assuming free, damped oscillations of the electrons, it is possible to obtain the differential equation governing these oscillations:

$$\ddot{\xi} - (2e^2/3mc^3)\ddot{\xi} + k_0^2c^2\xi = 0 \quad (1)$$

where ξ is the displacement of the electron per unit electric field, $-e$ its charge, m its mass, c the velocity of light in vacuum, and $k_0 = 2\pi\nu_0/c$ (ν_0 is the frequency of the undamped oscillations).

The scattered radiation is produced by the forced oscillations of the electrons caused by the incident radiation. The interaction of the incident radiation with the oscillators is small unless the incident frequency is near a natural frequency of the oscillators.

An expression describing forced oscillations due to an incident plane wave $E = \exp[ik(ct - x)]$ must include the force $-eE$ exerted by the field on the electrons. Equation (1) thus becomes

$$\ddot{\xi} - (2e^2/3mc^3)\ddot{\xi} + k_q^2c^2\xi = -(e/m)\exp[ik(ct - x)] \quad (2)$$

where the subscript q may refer to the K, L, M, etc absorption limits of the atom. (It should be noted that this treatment neglects the influence of adjacent electrons in the medium; in the x-ray region this influence can be shown to be comparatively small.)

The solution of Eq. (2) is of the form

$$\xi = a \exp [ik(ct - x)]$$

and when a is determined we obtain

$$\xi = - \frac{e \exp[ik(ct - x)]}{mc^2(k_q^2 - k^2) + 2e^2 ik^3/3} . \quad (3)$$

The polarization of the medium due to type- q electrons can thus be expressed as $P_q = -n_q e \xi$, where n_q is the number of type- q electrons per unit volume.

Using the relation between the dielectric constant κ and the polarization of the medium, and Eq. (3), we obtain

$$\kappa_q = 1 + \frac{4\pi n_q e^2}{mc^2(k_q^2 - k^2) + 2e^2 ik^3/3} . \quad (4)$$

Equation (4) indicates that the dielectric constant is complex and can be expressed as

$$\kappa = 1 - 2\delta - 2i\beta$$

where δ and β can be found from a comparison with Eq. (4).

From Maxwell's relation $v = c/\sqrt{\kappa}$, we see that a complex dielectric constant gives rise to a complex phase velocity. The significance of the complex nature of the phase velocity is most easily seen by discussing its reciprocal S_c :

$$S_c = 1/c(1 - 2\delta - 2i\beta)^{\frac{1}{2}} \approx 1/c(1 - \delta - i\beta) = S - iS_1 . \quad (5)$$

The equation of a plane wave moving through a medium is

$$\begin{aligned} E &= A \exp[i\omega(t - x/v)] = A \exp[i\omega(t - S_c x)] \\ &= A \exp[i\omega(t - Sx + iS_1 x)] = A \exp[i\omega(t - Sx)] \\ &\quad \times \exp(-\omega S_1 x) . \end{aligned} \quad (6)$$

It is thus seen that the imaginary part of the phase velocity

introduces an absorption coefficient characteristic of the medium and leads to an attenuation of the amplitude of the wave.

In dispersion theory the index of refraction which is the ratio of the phase velocities in vacuum and in the medium is, of course, also a complex quantity given by

$$n_c = n + in_i = 1 - \delta - i\beta.$$

A comparison of the experimentally measured index of refraction and its theoretically predicted value is thus a test of the correctness of the theory.

Experimental measurements of the index of refraction performed by a number of workers in the Twenties confirmed within the limits of experimental error the correctness of Lorentz's dispersion theory in regions in which the natural electronic frequencies of the medium can be neglected.

Agreement with the theory was found to be poor for the case of calcite when molybdenum $K\alpha$ and copper $K\alpha$ radiations were used.

However, the most definite need for a reconsideration of the Lorentz dispersion theory arose from its predictions regarding the linear absorption coefficient for x rays.

Squaring Eq. (6) and comparing it with the expression for the attenuation of a wave by a medium with a linear absorption coefficient μ_l^q , we obtain

$$\mu_l^q = 4\pi\beta_q/\lambda = \frac{8\pi n_q e^4 k^4}{3[\pi^2 c^4 (k_q^2 - k^2)^2 + 4e^4 k^6/9]}, \quad (7)$$

where β_q can be obtained from Eq. (4). The resultant expression

predicts a peak of μ_l about the natural frequency, whereas such a peak is not observed experimentally and the discontinuity actually occurs at a slightly higher frequency.

REVISED LORENTZ THEORY

In the revised Lorentz theory the absorption of x rays with a frequency higher than the critical absorption frequency, $\omega_q/2\pi$, is attributed to a set of "virtual" oscillators associated with the atom. These virtual oscillators have characteristic frequencies between ω_q and ∞ and those whose characteristic frequencies lie near that of the incident wave will contribute to its absorption. The number or "strength" of the virtual oscillators assigned to a given frequency is determined by a distribution function which must satisfy the equation

$$z_q = \int_{\omega_q}^{\infty} f(\omega_j) d\omega_j \quad (8)$$

where z_q is the number of electrons per atom associated with the q critical absorption frequency. By substituting expression (8) for n_q in (7), we obtain a contribution to the atomic absorption coefficient due to the q electrons

$$\mu_a^q = (8\pi/3) (e^2/m)^2 (\omega/c)^4 \int_{\omega_q}^{\infty} \frac{f(\omega_j) d\omega_j}{(\omega_j^2 - \omega^2)^2 + 4e^4 \omega^6 / 9m^2 c^6} \quad (9)$$

In view of the smallness of the term $4e^4 \omega^6 / 9m^2 c^6$, only small values of $(\omega_j^2 - \omega^2)$, i.e., values ω_j close to ω , will contribute effectively to the value of the integral. We can thus set $\omega_j = \omega$ in all cases where we are not dealing with a differ-

ence between the two, and we can approximate $f(\omega_j)$ by $f(\omega)$ neglecting the small variation of this value. We therefore, rewrite (9) as

$$\mu_a^q = (8\pi/3)(e^2/m)^2(\omega/c)^4 f(\omega)(1/4\omega^2) \int_{\omega_q}^{\infty} \frac{d\omega_j}{(\omega_j - \omega)^2 + e^4\omega^4/9m^2c^6} \cdot (10)$$

The integral can be evaluated as

$$(3mc^3/e^2\omega^2) \left[\tan^{-1} \frac{3(\omega_j - \omega)mc^3}{2e^2\omega^2} \right]_{\omega_q}^{\infty} = (3mc^3/e^2\omega^2) \left[\tan^{-1} \infty - \tan^{-1} \frac{3(\omega_q - \omega)mc^3}{e^2\omega^2} \right]$$

where $e^2\omega^2/3mc^3$ is a small quantity and $(\omega_q - \omega) 3mc^3/e^2\omega^2$ is, therefore, a large (negative) quantity, unless ω is very close to ω_q . Excluding the latter region, we can set $\tan^{-1}(\omega_q - \omega) 3mc^3/e^2\omega^2 = -\pi/2$, so that the value of the integral is $3\pi mc^3/e^2\omega^2$. Equation (10) thus becomes

$$\mu_a^q = (2\pi^2 e^2/mc) f(\omega) \cdot (11)$$

Combining (11) with (8), we have

$$\int_{\omega_q}^{\infty} \mu_a^q d\omega = (2\pi^2 e^2/mc) z_q \cdot (12)$$

By introducing in Eq. (12) the experimentally observed frequency variation of the absorption coefficient $\mu_a^q = k_q/\omega^3$ (k_q is a constant), one obtains

$$\mu_a^q = (4\pi^2 e^2/mc)(\omega_q^2/\omega^3) z_q, (13)$$

an expression which can be summed over the various atomic levels. Combining Eq. (13) and Eq. (11), we obtain

$$f(\omega_j) = 2\omega_q^2 z_q / \omega_j^3 \cdot (14)$$

ence between the two, and we can approximate $f(\omega_j)$ by $f(\omega)$ neglecting the small variation of this value. We therefore, rewrite (9) as

$$\mu_a^q = (8\pi/3)(e^2/m)^2(\omega/c)^4 f(\omega)(1/4\omega^2) \int_{\omega_q}^{\infty} \frac{d\omega_j}{(\omega_j - \omega)^2 + e^4\omega^4/9m^2c^6} \cdot (10)$$

The integral can be evaluated as

$$(3mc^3/e^2\omega^2) \left[\tan^{-1} \frac{3(\omega_j - \omega)mc^3}{2e^2\omega^2} \right]_{\omega_q}^{\infty} = (3mc^3/e^2\omega^2) \left[\tan^{-1} \infty - \tan^{-1} \frac{3(\omega_q - \omega)mc^3}{e^2\omega^2} \right]$$

where $e^2\omega^2/3mc^3$ is a small quantity and $(\omega_q - \omega)3mc^3/e^2\omega^2$ is, therefore, a large (negative) quantity, unless ω is very close to ω_q . Excluding the latter region, we can set $\tan^{-1}(\omega_q - \omega)3mc^3/e^2\omega^2 = -\pi/2$, so that the value of the integral is $3\pi mc^3/e^2\omega^2$. Equation (10) thus becomes

$$\mu_a^q = (2\pi^2 e^2/mc) f(\omega) \cdot (11)$$

Combining (11) with (8), we have

$$\int_{\omega_q}^{\infty} \mu_a^q d\omega = (2\pi^2 e^2/mc) z_q \cdot (12)$$

By introducing in Eq. (12) the experimentally observed frequency variation of the absorption coefficient $\mu_a^q = k_q/\omega^3$ (k_q is a constant), one obtains

$$\mu_a^q = (4\pi^2 e^2/mc)(\omega_q^2/\omega^3) z_q, (13)$$

an expression which can be summed over the various atomic levels. Combining Eq. (13) and Eq. (11), we obtain

$$f(\omega_j) = 2\omega_q^2 z_q / \omega_j^3 \cdot (14)$$

THE KRAMERS-KALLMAN-MARK THEORY OF THE REFRACTIVE INDEX

Using the expression for the refractive index

$$n_c = 1 - \delta - i\beta$$

and δ and β found according to the Lorentz theory, we find that the contribution to the complex refractive index due to the q electrons is

$$n_c^q = 1 + (2\pi e^2 n_q / m) (\omega_q^2 - \omega^2 + 2ie^2 \omega^3 / 3mc^3)^{-1} . \quad (15)$$

In the revised theory each electron is replaced by a distribution of virtual oscillators given by Eq. (14). The distribution per electron is $f(\omega_j)/z_q$, and

$$\mu_c^q = 1 + (4\pi e^2 n_q \omega_q^2 / m) \int_{\omega_q}^{\infty} \frac{d\omega_j}{\omega_j^3 (\omega_j^2 - \omega^2 + 2ie^2 \omega^2 / 3mc^3)} . \quad (16)$$

Integration yields new expressions for δ_q and β_q which were tabulated by Glocker and Schäfer (6). The validity of these equations at the absorption edge appears, however, unjustified, since Eq. (11) which, together with the experimental variation of μ_a^q , leads to Eq. (14), has been obtained under the assumption that ω is not very close to ω_q .

Investigations by Larsson, quoted in (5), on calcite near the K absorption edge of calcium showed that while the unmodified Lorentz formula did not agree with the experimental results, the modified theory accounted for them adequately. Some disagreement, particularly on the long-wavelength side of the absorption edge, was nevertheless noted and the discrepancy decreased somewhat when a value z_K smaller than

2 was used.

THE RELATION BETWEEN THE COMPLEX REFRACTIVE INDEX AND THE ATOMIC SCATTERING FACTOR, f_0

The equation of motion of a free, undamped electron is

$$a = \ddot{\xi} = -eE/m.$$

Hence the rate of loss of energy, w , by the electron is

$$dw/dt = -2e^4 E^2 / 3m^2 c^3 . \quad (17)$$

The acceleration of an electron executing forced, damped oscillations, obtained from the solution of Eq. (2) by differentiation, is

$$a = \ddot{\xi} = -k^2 c^2 \xi = -\omega^2 \xi .$$

The energy loss due to electromagnetic damping is, therefore,

$$dw/dt = -(2\omega^4/3c^3) |\xi e|^2 = -2\omega^4/3c^3 |p|^2 ,$$

where p is the dipole moment resulting from the displacement of a single electron.

The energy W radiated by the entire atom is

$$dW/dt = -(2\omega^4/3c^3) \left| \sum_q z_q p_q \right|^2 . \quad (18)$$

The polarization of the medium is given by

$$P = n_a \sum_q z_q p_q ,$$

where n_a is the number of atoms per unit volume.

The dielectric constant is thus

$$\kappa = 1 + (4\pi/E) n_a \sum_q z_q p_q ,$$

and

$$\delta + i\beta = n_a \sum_q z_q (\delta_q + i\beta_q) = -(2\pi/E) n_a \sum_q z_q p_q .$$

Equation (17) can now be written as

$$dW/dt = -(\omega^4 E^2 / 6\pi^2 c^3) \left| \sum_q z_q (\delta_q + i\beta_q) \right|^2.$$

Dividing this by Eq. (16), we obtain what is by definition f_0^2 at $\sin \theta = 0$

$$f_0^2 = (m^2 \omega^4 / 4\pi^2 e^4) \left| \sum_q z_q (\delta_q + i\beta_q) \right|^2; \quad (19)$$

this is the relation between the atomic scattering factor and the complex index of refraction. An investigation of the change of the atomic scattering factor with wavelength can therefore serve as a test of any dispersion theory.

FURTHER DEVELOPMENTS OF DISPERSION THEORY

Hönl (1) avoids the introduction in Eq. (15) of the virtual oscillator distribution obtained from the empirical λ^3 absorption law. In place of this he employs Sugiura's (7) quantum mechanical calculations of the oscillator strength of hydrogen, adapting these to the heavier atoms by suitable approximate corrections for screening and relativity effects. Hönl was thus able to calculate a distribution function per electron for the K electrons. By introducing this distribution in Eq. (15), he obtained expressions for δ_K and β_K , and hence for the variation of the atomic scattering factors with wavelength. In his more complete theory Hönl estimates the change of the correction to the atomic scattering factor as a function of the scattering angle in regions where the anomalous dispersion is due mainly to the K electrons. Hönl's results have been tabulated by James (8).

Hönl's theory has been extended by Eisenlohr and Müller (9) to include effects due to the L electrons. The calculations are unfortunately carried out only for tellurium and tungsten, and will have to be extended to other elements before further comparison with experimental results is possible.

Parratt and Hempstead (2), on the other hand, have approached the problem from a phenomenological point of view. From a survey of the literature they concluded that while the assumption of a λ^3 distribution of virtual oscillators makes

for easy integration of the expression for δ , $\lambda^{1/4}$ is probably more correct. They then proceeded to an integration of the dispersion expression for a general λ^{p_q} term where p_q is the fractional exponent corresponding to the q absorption edge. In this way it also became possible to include effects due to other electron shells. In order to evaluate the error due to the customary neglect of the damping factor, Parratt and Hempstead retained the damping factor in their calculations and subsequently concluded that its neglect is well justified except in cases where the incident wavelength is very close to an absorption discontinuity.

Dauben and Templeton (10) have used the methods of Parratt and Hempstead to calculate real and imaginary corrections to the atomic scattering factors of most elements for incident molybdenum, copper, and chromium $K\alpha$ radiation (for $\theta = 0$). Their calculations include effects due to the K, L, and M shells, and damping has been neglected. Templeton (11) has extended these calculations to the lighter elements, included effects due to the N shell, and calculated the variation of the corrections with $\sin \theta/\lambda$ by multiplying the contribution of each electron group by its individual form factor.

THE ANOMALOUS SCATTERING OF X RAYS

Experimental confirmation of the variation of the atomic scattering factors in the region of anomalous dispersion was first obtained by Mark and Szilard (12) who studied the intensity variation of the (111) reflection of RbBr with changing wavelength of the incident radiation. The structure factor of the (111) reflection of RbBr is a term involving the difference of the atomic scattering factors of the two elements, and the (111) reflection thus appears only when these are unequal. Mark and Szilard demonstrated that this occurs in the region of anomalous dispersion when SrK α radiation, with a wavelength close to and between the absorption edges of Rb and Br, is employed.

The above qualitative demonstration was soon followed by a series of measurements of atomic scattering factors using various incident wavelengths. The first of these by Armstrong (13) for copper using CuK α and MoK α radiation indicated approximate agreement with values calculated from Hönl's theory. These measurements were extended by Wyckoff (14) who measured the atomic scattering factors of nickel and oxygen in NiO, and later used powders to measure those of nickel, copper, and iron. These results are in general agreement with Hönl's theory. Bradley and Hope (15) used powdered FeAl to find the scattering factors of iron and aluminum. Glocker and Schäfer (6) also investigated powdered iron with an admixture of aluminum. This method of admixing a standard powder was employed

by Rusterholz (16) for measurements of the scattering factor of copper on the long-wavelength side of the K edge. Brindley and Spiers (17) used this method to measure the scattering factors of copper and nickel. The values obtained by them were somewhat lower than those predicted by Hönl. Brentano and Baxter (18) employed the method of mixed powders to determine the scattering factors of tungsten in the neighborhood of the L absorption edges. Eisenlohr and Müller (9) compared the results of these measurements with their theoretical work on the dispersion due to the L electrons. The experimental values fall in general below the theoretical curve on the short-wavelength side, while the agreement on the long-wavelength side is quite good.

Roof (26) has recently investigated the dispersion of the atomic scattering factors of Th, U, and Pu with MoK α , CuK α , FeK α , and CrK α radiations which are close to the L and M absorption edges of these elements. He reported qualitative agreement with Templeton's calculated dispersion corrections.

In general, measurements of the atomic scattering factors are subject to considerable uncertainties owing to possible errors in allowing for absorption in the powders and for the effect of the temperature motion of the atoms in the crystal. Errors may also be introduced by an incorrect determination of absolute intensities. When single crystals are used, extinction can affect the results appreciably.

A method which avoids almost all of these sources of error is based on the anomalous scattering of x rays by non-

centrosymmetric crystals.

The amplitude F_{\pm} of x rays diffracted by a crystal containing atoms that show appreciable dispersive effects and others that do not, can be written as

$$F_{\pm} = A_n + i\sigma B_n + (C_d + i\sigma D_d)(f_d + \Delta f' + i\Delta f''),$$

where the plus and minus subscripts of F refer to the (hkl) and $(\bar{h}\bar{k}\bar{l})$ reflections respectively, A_n and B_n are the structure-factor components due to the nondispersive element, $\sigma = +1$ and -1 for (hkl) and $(\bar{h}\bar{k}\bar{l})$ respectively, $C_d f_d = A_d$ and $D_d f_d = B_d$ are the structure-factor components of the dispersive atom, where f_d is the atomic scattering factor of the atom at rest to which the dispersion corrections $\Delta f'$ and $i\Delta f''$ have to be added, and where C_d and D_d contain the temperature factors of the dispersive element. The amplitude can be written as

$$\begin{aligned} F_{\pm} &= (A_n + A_d + C_d \Delta f' - \sigma D_d \Delta f'') \\ &\quad + i\sigma(B_n + B_d + D_d \Delta f' + \sigma C_d \Delta f'') \\ &= (A - \sigma D_d \Delta f'') + i\sigma(B + \sigma C_d \Delta f''), \end{aligned}$$

where $A_n + A_d + C_d \Delta f' = A$ and $B_n + B_d + D_d \Delta f' = B$.

The intensities I_+ and I_- of the (hkl) and $(\bar{h}\bar{k}\bar{l})$ reflections are therefore

$$\begin{aligned} I_+ &= F_+ F_+^* = [(A - D_d \Delta f'') + i(B + C_d \Delta f'')] \\ &\quad \times [(A - D_d \Delta f'') - i(B + C_d \Delta f'')] \\ &= (A - D_d \Delta f'')^2 + (C_d \Delta f'' + B)^2 \\ I_- &= F_- F_-^* = (A + D_d \Delta f'')^2 + (B - C_d \Delta f'')^2, \end{aligned}$$

and are thus found not to obey Friedel's law.

Forming the ratio

$$\frac{\Delta I}{I_{av}} = \frac{I_+ - I_-}{(I_+ + I_-)/2} = \frac{8BC_d\Delta f'' - 8AD_d\Delta f''}{A^2 + B^2 + D_d^2\Delta f''^2 + C_d^2\Delta f''^2},$$

we find that it is a function of the atomic scattering factors and of the dispersion corrections. It will be noted that the experimentally observed ratio $\Delta I/I_{av}$ can be directly compared with the theoretically predicted values, requiring no correction for absorption [if it can be assumed that the absorption is identical for (hkl) and $(\bar{h}\bar{k}\bar{l})$ reflections], no θ -dependent corrections, and no conversion to absolute intensities. The assumption that the temperature factors in the numerator and in the denominator of the ratio cancel out introduces an error, particularly at large values of $\sin \theta/\lambda$, since it is equivalent to assigning to each atom in the lattice the same "average" temperature factor (cf. Table 3).

Nishikawa and Matukawa (19) and Coster, Knol, and Prins (20) were the first to investigate the inequality of the intensities of the (111) and the $(\bar{1}\bar{1}\bar{1})$ reflections of cubic zinc sulfide.

Harrison, Jeffrey, and Townsend (21) used the anomalous scattering of MoK α radiation to investigate the agreement of Hönl's theory with the experimentally observed intensities of the (hkl) and $(h\bar{k}\bar{l})$ reflections of ZnO crystals. Their results indicated considerable disagreement with the theory.

In a continuation of this study Townsend, Jeffrey, and Panagis (3) investigated single crystals of cubic zinc sul-

fide. Cubic zinc sulfide (sphalerite) has a face-centered lattice with four molecules per unit cell. The special positions of the atoms are determined by the space group $F\bar{4}3m$ to be at (000) and $(1/4, 1/4, 1/4)$ and at other lattice-related positions. The structure factor is found to be

$$F = 4[f'_{Zn} + i\Delta f''_{Zn} + (f'_S + i\Delta f''_S) \exp(\pi i H/2)]$$

where $f'_{Zn,S} = f_{Zn,S} + \Delta f'_{Zn,S}$ and $H = h + k + l$.

This reduces to

$$F = 4(f'_{Zn} + i\Delta f''_{Zn} + f'_S + i\Delta f''_S) \quad \text{when } H = 4n$$

$$F = 4(f'_{Zn} + i\Delta f''_{Zn} - f'_S - i\Delta f''_S) \quad \text{when } H = 2n$$

$$F = 4(f'_{Zn} + i\Delta f''_{Zn} + \sigma f'_S - \sigma \Delta f''_S) \quad \text{where } \sigma = +1 \text{ if } H = 4n + 1 \\ \text{and } \sigma = -1 \text{ if } H = 4n - 1 \\ (n = 0, \pm 1, \pm 2, \pm 3, \dots).$$

The intensities are

$$I = 16[(f'_{Zn} + f'_S)^2 + (\Delta f''_{Zn} + \Delta f''_S)^2] \quad \text{when } H = 4n$$

$$I = 16[(f'_{Zn} - f'_S)^2 + (\Delta f''_{Zn} - \Delta f''_S)^2] \quad \text{when } H = 2n$$

$$I = 16[(f'_{Zn} - \sigma f'_S)^2 + (\Delta f''_{Zn} + \sigma \Delta f''_S)^2] \quad \text{where } \sigma = +1 \text{ if } H = 4n + 1 \\ \sigma = -1 \text{ if } H = 4n - 1.$$

The (hkl) and $(\bar{h}\bar{k}\bar{l})$ reflections with h , k , and l odd are thus seen to differ in their intensities, and the ratio of this difference to their average intensity is found to be

$$\frac{\Delta I}{I_{av}} = \frac{4(\Delta f''_S f'_{Zn} - \Delta f''_{Zn} f'_S)}{f'^2_{Zn} + f'^2_S + \Delta f''^2_{Zn} + \Delta f''^2_S} \quad (20)$$

Unlike in the case of ZnO, Townsend, Jeffrey, and Panagis (3) found that the experimental values obtained for ZnS with MoK α and CuK α radiation are in essential agreement with theoretical calculations using angle-independent anomalous-dispersion corrections for the atomic scattering factors. They also found that a clear choice between the values based on the work of Hönl and those based on the work of Parratt and Hempstead was impossible because of the scatter of experimental values.

This work on ZnS was extended by Friedman (4) to include a larger number of reflections. Friedman's data are in agreement with those of Townsend, Jeffrey, and Panagis and the scatter of the experimental results is smaller. Nevertheless, no clear choice between the two sets of theoretical corrections could be made.

The first portion of this thesis is a repetition of the work on cubic ZnS extended to include more reflections and measurements with CrK α radiation. Similar measurements using CuK α and CrK α radiation were then performed on the isostructural boron phosphide and attempts were made to obtain experimental values of the dispersion corrections to the atomic scattering factors.

EXPERIMENTAL WORK

THE ANOMALOUS SCATTERING OF MOLYBDENUM K_{α} RADIATION BY CUBIC ZINC SULFIDE

The natural crystals of the investigated cubic zinc sulfide (sphalerite) originated in Santander, Spain. The golden-colored transparent samples were obtained from the Museum of Natural History in New York City (file no. 7090). Their color and transparency are evidence of their comparatively high purity; sphalerite from Santander is reported in Dana's System of Mineralogy (22) to contain 0.45 percent tin and 0.40 percent iron impurity. An x-ray fluorescence analysis of a powder specimen of the material indicated the presence of less than one percent of iron. No other impurities with atomic number greater than 19 were detected (4).

Several crystals were ground to spherical shape using a diamond-lined sphere grinder (4). The diameter of the sphere selected for this work (referred to below as ZnS #1) was 0.384 ± 0.004 mm. This sphere was mounted with shellac on a fine glass fiber drawn from the soft glass of the capillary tubes commonly used in the preparation of Debye-Scherrer samples. Rotation photographs confirmed that the sphere consisted of a single crystal; no strain was apparent.

The intensities of 36 sets of reflections with all indices odd and of 12 sets with all indices even were measured on the General Electric XRD-5 Single Crystal Orienter with a stationary scintillation counter and stationary crystal.

A zirconium filter, augmented by electronic pulse-height selection, was used to discriminate against unwanted wavelengths.

Of each investigated set with hkl odd the intensities of at least four reflections were measured by noting the time required for the scaler to accumulate a given number of counts; of sets with hkl even two equivalent reflections were similarly measured. With increasing θ , the number of counts required to accumulate was gradually reduced from 100 000 to 10 000. The background on both sides of each peak was measured similarly, except that the number of background counts required to accumulate was varied from 1000 to 400. Measurements of the intensity at the peak maximum (the $K\alpha_1$ peak in the region where it was resolved from the $K\alpha_2$ peak) as well as of the background on each side were repeated at least three times.

Tables 1 and 2 list the averages of the repeated measurements of the peak intensity (converted to counts per second) after subtraction of the background which was taken to be the average of the measurements on both sides of the peak. The corresponding average deviations from the mean are indicated in Table 1. The deviations of the absolute values of $\Delta I/I_{av}$ from zero for reflections with hkl even (Table 2) serve as an additional measure of the magnitude of the experimental errors.

In the system of indexing employed all reflections with $h + k + l = 4n + 1$ were consistently found to be more

intense than those with $h + k + l = 4n - 1$.

Table 3 lists the experimental and theoretical values of $\Delta I/I_{av}$. The theoretical values were calculated from Eq. (20) using the atomic scattering factor for zinc calculated on the Thomas-Fermi-Dirac statistical model (11) and the atomic scattering factor for sulfur calculated from self-consistent and variational wave functions (11). The dispersion corrections used were those listed in the International Tables for X-Ray Crystallography (11) based on the calculations of Dauben and Templeton (10), and those based on the calculations of Hönl and tabulated by James (8).

The values of $(\Delta I/I_{av})_{obs}$ listed in Tables 2 and 3 are plotted in Fig. 1 as a function of $\sin \theta$. In Fig. 2 these values (averaged whenever two or more reflections occurred at the same value of $\sin \theta$) are plotted together with the theoretical curves calculated with the two sets of corrections. A third curve was calculated by applying Templeton's (11) dispersion corrections and Miller's (23) temperature factors ($B_{Zn} = 0.90 \text{ \AA}^2$, $B_S = 0.60 \text{ \AA}^2$) to the atomic scattering factors. The third curve shows clearly the error introduced by assuming $\Delta I/I_{av}$ to be independent of temperature effects, and improves the agreement between theory and experiment at large Bragg angles.

Table 1. Peak intensities of reflections with hkl odd (ZnS #1 with $\text{MoK}\alpha$ radiation).

hkl	Counts/sec	a.d.	hkl	Counts/sec	a.d.
111	11687	36	335	954	8
1 $\bar{1}\bar{1}$	11616	36	533	969	8
11 $\bar{1}$	13039	93	33 $\bar{5}$	1140	8
$\bar{1}$ 11	12854	93	$\bar{5}$ 33	1124	8
113	5328	24	551	717	8
311	5375	24	155	732	8
11 $\bar{3}$	4990	28	55 $\bar{1}$	868	2.5
$\bar{3}$ 11	4934	28	$\bar{1}$ 55	863	2.5
331	3049	31	117	830	1
133	3104	31	711	828	1
33 $\bar{1}$	3360	8	$\bar{1}$ 17	694	3
$\bar{1}$ 33	3344	8	7 $\bar{1}$ 1	700	3
333	2235	8	355	631	0.5
3 $\bar{3}$ $\bar{3}$	2219	8	535	630	0.5
33 $\bar{3}$	2056	13	$\bar{3}$ 55	524	
$\bar{3}$ 33	2031	13	5 $\bar{3}$ 5	524	
115	1958	7	317	509	
511	1971	7	173	509	
11 $\bar{5}$	2241	28	31 $\bar{7}$	628	2
$\bar{5}$ 11	2296	28	1 $\bar{7}$ 3	632	2
531	1597	5	337	483	1.5
153	1606	5	373	486	1.5
53 $\bar{1}$	1404	12	33 $\bar{7}$	397	2
3 $\bar{1}$ 5	1380	12	$\bar{7}$ 33	393	2

Table 1 (continued)

hkl	Counts/sec	a.d.	hkl	Counts/sec	a.d.
555	283	3	575	186	1
$\bar{5}5\bar{5}$	289	3	755	184	1
$5\bar{5}5$	371	1	$5\bar{5}\bar{7}$	147.5	0.4
$\bar{5}55$	369	1	$\bar{7}55$	146.8	0.4
751	366	0.5	933	140.5	0.1
517	365	0.5	393	140.7	0.1
$7\bar{5}\bar{1}$	293		$3\bar{3}\bar{9}$	180.2	0.8
$5\bar{1}\bar{7}$	293		$\bar{9}33$	181.8	0.8
119	219	0.5	773	144.1	0.3
191	220	0.5	737	143.6	0.3
$\bar{1}19$	280	0.5	$7\bar{7}\bar{3}$	115.3	0.2
$9\bar{1}\bar{1}$	281	0.5	$\bar{3}77$	116.6	0.2
753	213		951	111.42	0.38
375	213		195	112.08	0.38
$7\bar{5}\bar{3}$	284	1	$9\bar{5}\bar{1}$	145.16	0.66
$\bar{3}7\bar{5}$	286	1	$\bar{1}95$	146.49	0.66
319	212	1	539	113.79	0.05
931	214	1	953	113.88	0.05
$\bar{3}19$	172	0.5	$5\bar{3}\bar{9}$	90.24	0.48
$9\bar{3}\bar{1}$	173	0.5	$\bar{9}53$	91.19	0.48
771	142	0.5	775	80.46	0.16
177	141	0.5	577	80.78	0.16
$7\bar{7}\bar{1}$	130	0.5	$7\bar{7}\bar{5}$	108.69	0.18
$\bar{1}77$	181	0.5	$\bar{5}77$	108.34	0.18

Table 1 (concluded)

hkl	Counts/sec	a.d.	hkl	Counts/sec	a.d.
11 1 1	111.22	0.33	3 5 11	54.80	0.13
1 11 1	110.57	0.33	11 3 5	54.55	0.13
11 1 $\bar{1}$	96.02	0.02	3 5 $\bar{1}\bar{1}$	73.42	0.20
$\bar{1}$ 11 1	95.98	0.02	$\bar{1}\bar{1}$ 3 5	73.81	0.20
559	70.12	0.23	991	52.17	0.01
955	70.58	0.23	199	52.16	0.01
55 $\bar{9}$	93.61	0.09	99 $\bar{1}$	65.63	0.18
$\bar{9}$ 55	93.78	0.09	$\bar{1}$ 99	65.27	0.18
971	94.06	0.04	939	70.73	0.12
197	94.14	0.04	993	70.97	0.12
97 $\bar{1}$	72.72	0.36	99 $\bar{3}$	54.84	0.38
$\bar{1}$ 97	72.00	0.36	$\bar{3}$ 99	55.60	0.38
973	65.56	0.17	1 1 13	52.84	0.31
397	65.22	0.17	13 1 1	52.23	0.31
97 $\bar{3}$	86.90	0.08	$\bar{1}$ 1 13	66.38	0.06
$\bar{3}$ 97	87.05	0.08	13 $\bar{1}$ 1	66.25	0.06
7 $\bar{7}$ $\bar{7}$	81.78	0.40	995	47.54	0.10
$\bar{7}$ $\bar{7}$ $\bar{7}$	82.57	0.40	599	47.34	0.10
77 $\bar{7}$	66.43	0.20	99 $\bar{5}$	65.09	0.50
$\bar{7}$ 77	65.84	0.20	9 $\bar{5}$ 9	66.09	0.50
5 1 11	80.45	0.18	3 3 13	47.91	0.07
11 5 1	80.09	0.18	13 3 3	47.78	0.07
5 1 $\bar{1}$	58.94	0.03	$\bar{3}$ 3 13	62.55	0.16
11 $\bar{5}$ 1	59.00	0.03	13 $\bar{3}$ 3	62.87	0.16

Table 2. Intensities of reflections with hkl even (ZnS #1 with MoK α radiation) and the observed absolute values of $\Delta I/I_{av}$

hkl	$\sin \theta$	Counts/sec	$100(\Delta I/I_{av})_{obs}$
200	0.13110	3323	1.7
020	0.13110	3380	
220	0.18550	10083	0.9
$\bar{2}\bar{2}0$	0.18550	9990	
400	0.26253	5638	0.8
040	0.26253	5682	
440	0.37104	2844	0.6
$\bar{4}\bar{4}0$	0.37104	2826	
620	0.41485	1984	1.4
206	0.41485	2012	
800	0.52480	822.6	0.5
080	0.52480	818.2	
660	0.55663	645.8	1.3
$\bar{6}\bar{6}0$	0.55663	637.5	
844	0.64275	273.9	2.1
484	0.64275	268.2	
880	0.74218	156.4	0.6
$\bar{8}\bar{8}0$	0.74218	155.4	
12 0 0	0.78720	123.6	0.5
0 12 0	0.78720	123.0	
12 4 0	0.82978	106.1	1.0
4 0 12	0.82978	105.0	
10 10 0	0.92772	104.1	0.7
$\bar{1}\bar{0} \bar{1}\bar{0} 0$	0.92772	103.4	

Table 3. Experimental and theoretical values of $\Delta I/I_{av}$ for zinc sulfide (MoK α radiation).

hkl	sin θ	100($\Delta I/I_{av}$) _{obs}	Hönl	Theoretical values	
				Dauben and Templeton	Dauben and Templeton*
111	0.11362	10.6 \pm 0.8	6.98	7.49	7.52
113	0.21757	7.56 \pm 0.7	8.33	8.72	
133	0.28594	8.65 \pm 1.0	9.88	10.18	
333	0.34087	8.57 \pm 0.7	11.31	11.58	12.05
115	0.34087	14.4 \pm 1.1	11.31	11.58	
135	0.38810	14.0 \pm 0.9	12.58	12.78	
335	0.43017	16.2 \pm 1.1	13.72	13.88	14.77
155	0.46848	17.7 \pm 1.1	14.69	14.81	
117	0.46848	17.3 \pm 0.4	14.69	14.81	
355	0.50388	18.5 \pm 0.1	15.55	15.49	16.81
137	0.50388	21.2 \pm 0.4	15.55	15.49	
337	0.53696	20.5 \pm 0.6	16.20	15.98	
555	0.56811	25.6 \pm 1.0	16.68	16.19	18.04
157	0.56811	22.1 \pm 0.2	16.68	16.19	
119	0.59764	24.3 \pm 0.3	17.06	16.46	
357	0.59764	28.9 \pm 0.4	17.06	16.46	
139	0.62578	20.7 \pm 0.6	17.56	16.69	
177	0.65271	24.1 \pm 0.4	18.02	16.91	19.63
557	0.65271	22.8 \pm 0.6	18.02	16.91	
339	0.65271	25.1 \pm 0.5	18.02	16.91	
377	0.67857	21.5 \pm 0.2	18.40	17.63	
159	0.67857	26.5 \pm 0.6	18.40	17.63	

*Corrected for thermal effects.

Table 3 (continued)

hkl	sin θ	100($\Delta I/I_{av}$) _{obs}	Theoretical values		Dauben and Templeton*
			Hönl	Dauben and Templeton	
359	0.70348	22.6 \pm 0.2	18.71	18.12	
577	0.72754	29.5 \pm 0.3	18.85	18.65	
1 1 11	0.72754	14.4 \pm 1.1	18.85	18.65	
559	0.75082	28.5 \pm 0.3	19.05	19.00	
179	0.75082	26.1 \pm 0.4	19.05	19.00	
379	0.77341	28.3 \pm 0.3	19.31	19.53	
777	0.79536	21.6 \pm 0.6	19.52	19.70	24.66
1 5 11	0.79536	30.6 \pm 0.3	19.52	19.70	
3 5 11	0.81671	29.5 \pm 0.4	19.74	20.17	
199	0.83752	22.6 \pm 0.3	20.02	21.00	
399	0.85783	24.8 \pm 0.6	20.23	21.53	
1 1 13	0.85783	23.2 \pm 0.5	20.23	21.53	
599	0.89707	32.1 \pm 0.9	20.61	22.34	30.15
3 3 13	0.89707	26.9 \pm 0.3	20.61	22.34	

*Corrected for thermal effects.

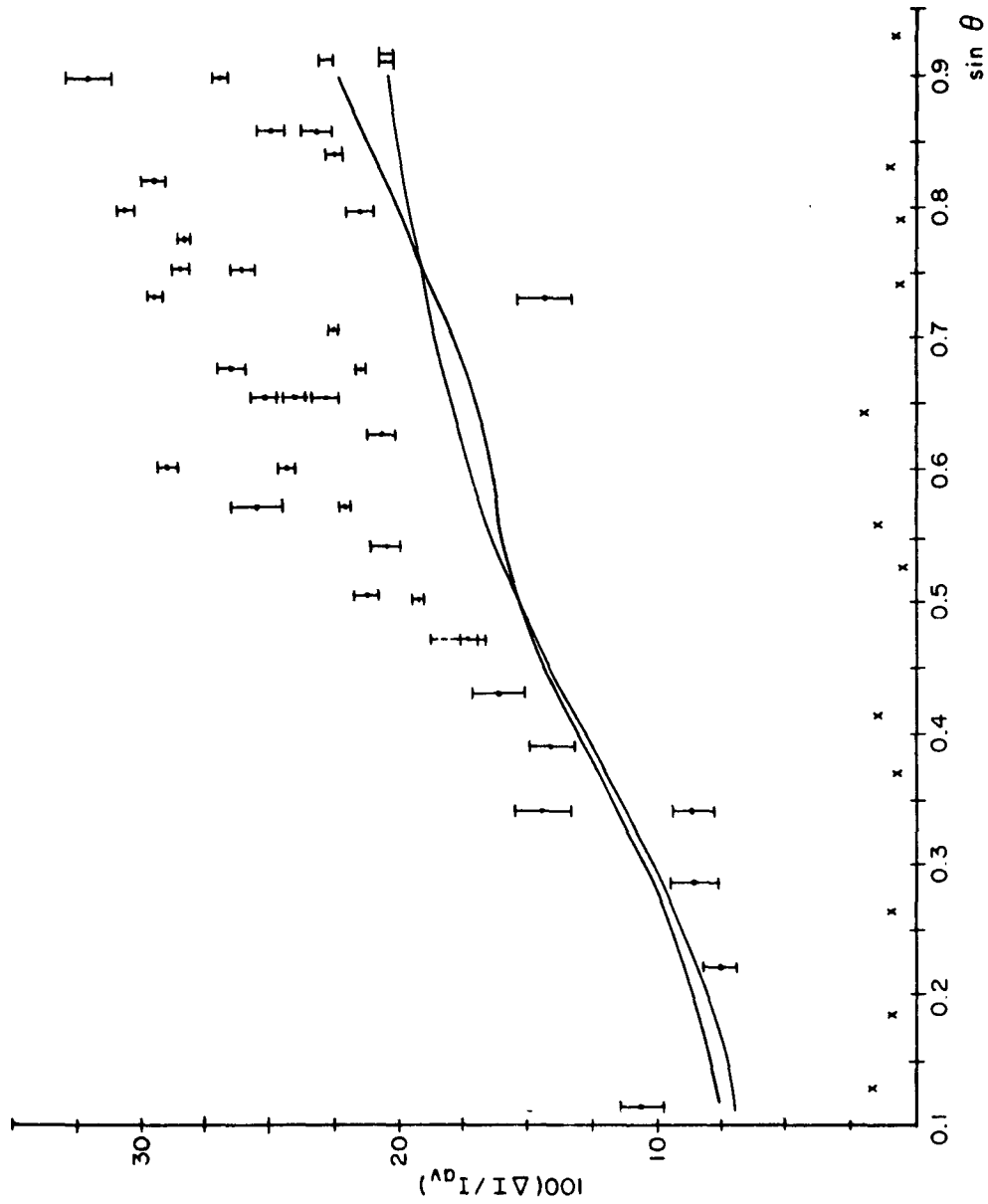


Fig. 1. $\Delta I/I_{av}$ as a function of $\sin \theta$ for ZnS with MoK α radiation. Curve I -- $\Delta I/I_{av}$ calculated using the dispersion corrections from the International Tables(11). Curve II -- $\Delta I/I_{av}$ calculated using H \ddot{o} nl's corrections. x -- absolute values of $\Delta I/I_{av}$ of selected all-even reflections.

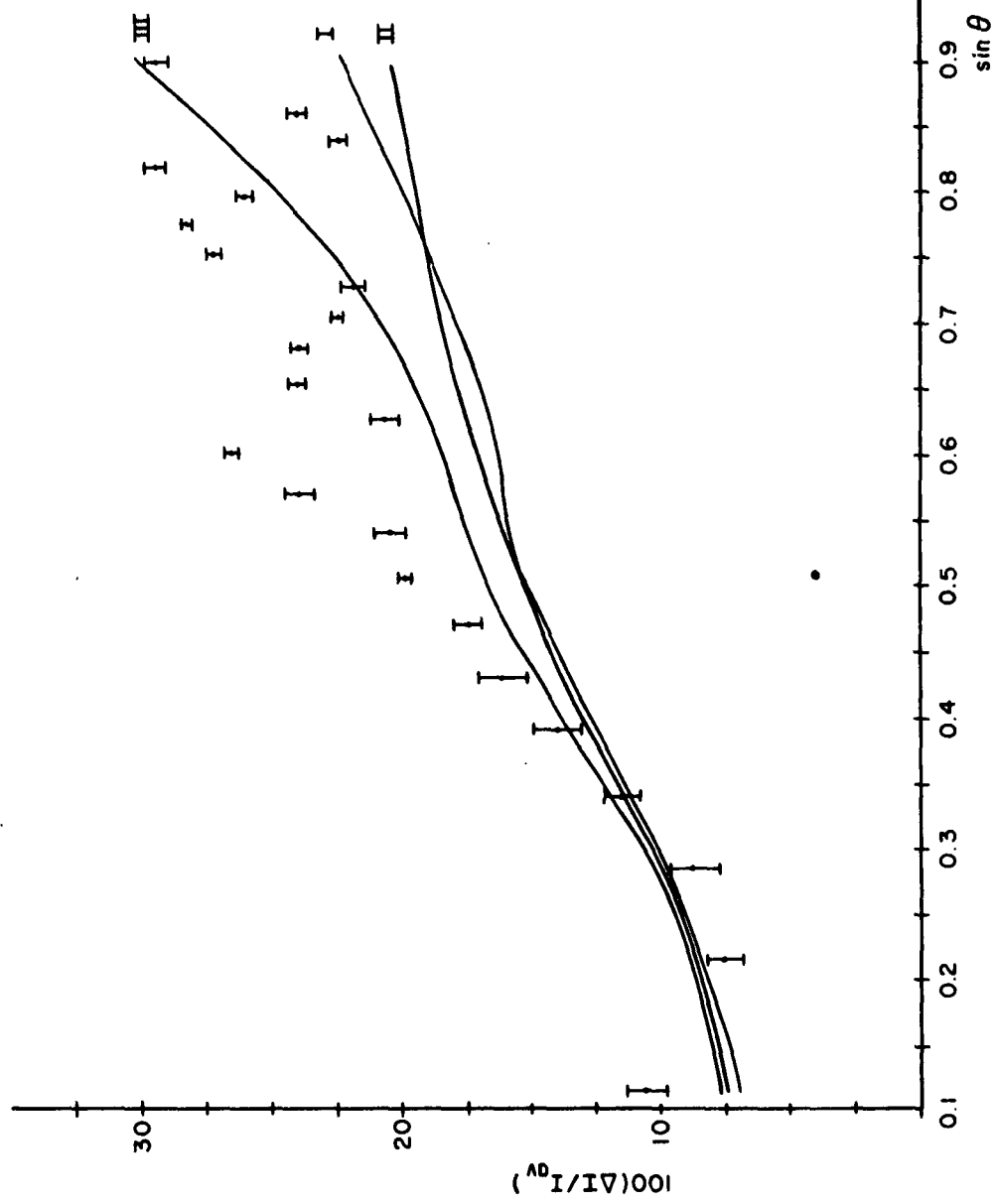


Fig. 2. Averaged values of $\Delta I/I_{av}$ as a function of $\sin \theta$ for ZnS with MoK α radiation. Curve I and II are the same as in Fig. 1. Curve III -- $\Delta I/I_{av}$ calculated using Templeton's dispersion corrections and corrected for temperature effects.

THE ANOMALOUS SCATTERING OF COPPER K_{α} RADIATION BY CUBIC
ZINC SULFIDE

The first set of measurements with CuK_{α} radiation (Table 4) was obtained with the crystal described in the previous section (ZnS #1). In view of the fact that the results of these measurements were in disagreement with previous results (3,4), an additional crystal (ZnS #2) with a diameter of 0.491 ± 0.002 mm was selected from those previously ground, and the integrated intensities of four sets of reflections with all indices odd were measured (Table 5). The experimental and theoretical values of $\Delta I/I_{av}$ are summarized in Table 6 and plotted as a function of $\sin \theta$ in Figs. 3 and 4.

In terms of the hkl indices used in this investigation, it was found that with copper radiation all reflections with $h+k+l = 4n+1$ were less intense than those with $h+k+l = 4n-1$. It will be recalled that the opposite was true for molybdenum radiation. This reversal of the relative intensities of the two sets of reflections is due to the change in the relative values of $\Delta f''_{Zn}$ and $\Delta f''_S$ for the two radiations.

In order to minimize possible errors in the subtraction of background counts, Ross filters (cf. Appendix) were employed. The integrated intensities were obtained by subtracting the number of counts recorded by the scaler in the course of a $\theta-2\theta$ scan with the cobalt-oxide filter from the number of counts recorded in the course of an identical scan with the nickel-and-aluminum filter. The scanning rate was $2^{\circ}2\theta$ and $1^{\circ}2\theta$ per minute for ZnS #1 and ZnS #2 respectively, and the

angular range scanned in each case was 3 and 1/3 degrees 2θ . Each measurement was repeated at least three times.

After being filtered, the radiation entered the proportional counter. The resultant pulses were preamplified and then additionally amplified by a linear amplifier. In the case of ZnS #1 use was also made of pulse-height selection to discriminate against unwanted wavelengths.

Although only intensities of reflections with hkl odd are presented in the Tables, a number of equivalent reflections with hkl even was checked. In general these were found to be equal within experimental error.

ATTEMPT TO OBTAIN EXPERIMENTAL VALUES OF THE IMAGINARY
DISPERSION CORRECTIONS $\Delta f''_{Zn}$ AND $\Delta f''_S$

The fact that anomalous scattering is due to the imaginary part of the dispersion correction suggested that the experimental data might yield experimental values of the corrections $\Delta f''_{Zn}$ and $\Delta f''_S$.

Substituting in Eq. (20) the experimental values of $\Delta I/I_{av}$, we obtain a set of equations

$$\Delta f''_S f'_{Zn} - \Delta f''_{Zn} f'_S = 1/4(\Delta I/I_{av})_{obs} \times [f'^2_{Zn} + f'^2_S + \Delta f''^2_{Zn} + \Delta f''^2_S] \quad (21)$$

Substituting in these equations the values of $f'_{Zn} = f_{Zn} + \Delta f'_{Zn}$ and f'_S found in the International Tables (11) and using as a

first approximation in the right-hand side the values for $\Delta f''_{Zn}$ and $\Delta f''_S$ found in the Tables, we obtained a set of linear simultaneous equations. A least-square treatment of this set yielded preliminary values of $\Delta f''_{Zn}$ and $\Delta f''_S$. These were then substituted in the right-hand side of Eq. (21) and the least-square procedure was repeated, yielding the following values:

$$\Delta f''_{Zn} = 2.8 \pm 1.2$$

$$\Delta f''_S = 1.9 \pm 0.5$$

The errors in these values were estimated from the largest error limits in the averaged values of $\Delta I/I_{av}$.

Some justification for using the theoretical real dispersion corrections, which may themselves be in error, in Eqs. (21) can be found when the variation of $\Delta I/I_{av}$ with $f'_{Zn,S}$ and $\Delta f''_{Zn,S}$ is investigated. Rewriting Eq. (20) in the form

$$R = \Delta I/I_{av} = 4(f'_{Zn}\Delta f''_S - f'_S\Delta f''_{Zn})/D$$

$$D = f'^2_{Zn} + f'^2_S + \Delta f''^2_{Zn} + \Delta f''^2_S,$$

we consider R a function of $f'_{Zn} = f_{Zn} + \Delta f'_{Zn}$, f'_S , $\Delta f''_{Zn}$, and $\Delta f''_S$, and calculate the differential

$$dR = \frac{\partial R}{\partial f'_{Zn}} d(f'_{Zn}) + \frac{\partial R}{\partial f'_S} d(f'_S) + \frac{\partial R}{\partial \Delta f''_{Zn}} d(\Delta f''_{Zn}) + \frac{\partial R}{\partial \Delta f''_S} d(\Delta f''_S).$$

The symmetric form of Eq. (20) enables us to restrict ourselves to a consideration of only two terms of the above

expression.

Thus,

$$\begin{aligned}
 dR = & [4(D\Delta f_S'' - 2f_{Zn}^{\prime 2}\Delta f_S'' + 2f_S^{\prime}f_{Zn}^{\prime}\Delta f_{Zn}'')/D^2]d(f_{Zn}^{\prime}) \\
 & + [4(2f_S^{\prime}\Delta f_{Zn}''^2 - 2f_{Zn}^{\prime}\Delta f_S''\Delta f_{Zn}'' - Df_S^{\prime})/D^2]d(\Delta f_{Zn}'') \\
 & + \text{two similar terms.}
 \end{aligned}$$

Comparing the numerators of the two terms, and remembering that $\Delta f''$ is, especially at small values of $\sin \theta$, much smaller than Df' , it is seen that R changes much more rapidly with a change in $\Delta f''$ than with a comparable change in f' .

Table 4. Integrated intensities of reflections with hkl odd (ZnS #1 with $CuK\alpha$ radiation).

hkl	Counts	a.d.	hkl	Counts	a.d.
$\bar{1}11$	85862	172	$3\bar{3}\bar{3}$	35213	276
$1\bar{1}1$	85670		$\bar{3}3\bar{3}$	34745	
$11\bar{1}$	85378		$\bar{3}\bar{3}3$	34440	
$\bar{1}\bar{1}1$	90566	334	$\bar{3}33$	36604	205
$1\bar{1}\bar{1}$	90163		$3\bar{3}\bar{3}$	37013	
$\bar{1}1\bar{1}$	89613				
$\bar{3}11$	54317	775	$5\bar{1}\bar{1}$	35235	149
$1\bar{3}1$	53170		$\bar{1}5\bar{1}$	35532	
$11\bar{3}$	55043		$\bar{5}11$	33797	94
$3\bar{1}\bar{1}$	51018	655	$1\bar{5}1$	33610	
$\bar{1}3\bar{1}$	52360				
$\bar{1}\bar{1}3$	52624				
311	50414	1599	$5\bar{3}\bar{1}$	40910	88
131	54307		$\bar{1}5\bar{3}$	41119	
113	51003		$\bar{3}\bar{1}5$	40930	
$31\bar{1}$	57560	347	$\bar{5}31$	43421	311
$\bar{1}31$	56580		$1\bar{5}3$	42800	
$1\bar{1}3$	56977				
$\bar{3}3\bar{1}$	40987	680	$\bar{3}\bar{3}5$	72737	667
$\bar{1}\bar{3}\bar{3}$	39773		$5\bar{3}\bar{3}$	73543	
$3\bar{1}\bar{3}$	41617		$\bar{3}5\bar{3}$	72435	
$3\bar{3}1$	37997	259	$3\bar{3}\bar{5}$	71966	822
$13\bar{3}$	38607		$\bar{5}33$	70357	
$\bar{3}13$	38053		$3\bar{5}3$	69875	

Table 5. Integrated intensities of reflections with hkl odd (ZnS #2 with $\text{CuK}\alpha$ radiation).

hkl	Counts	a.d.	hkl	Counts	a.d.
$1\bar{1}1$	180820	884	$33\bar{1}$	102243	256
$11\bar{1}$	179053		$\bar{1}33$	102691	
$\bar{1}\bar{1}1$	193946	193	$3\bar{1}3$	101986	
$\bar{1}1\bar{1}$	194332		$\bar{3}5\bar{3}$	102138*	76
$\bar{1}\bar{1}3$	118707	357	$5\bar{3}\bar{3}$	102394*	
$\bar{1}3\bar{1}$	119420		$33\bar{5}$	97177*	946
$1\bar{3}1$	127710	744	$\bar{5}33$	98689*	
$11\bar{3}$	129197		$3\bar{5}3$	95942*	
313	107935	1378			
133	110477				
331	106819				

*The 335 reflections were measured, unlike the other reflections, with pulse-height discrimination.

Table 6. Experimental and theoretical values of $\Delta I/I_{av}$ for zinc sulfide (CuK α radiation).

hkl	sin θ	100($\Delta I/I_{av}$) _{obs}		Average values		Theoretical values Dauben and Templeton
		ZnS #1	ZnS # 2			
111	0.24666	5.1 \pm 0.4	7.6 \pm 0.5	6.4 \pm 0.3	2.33	
113	0.47163	6.8 \pm 1.8	7.6 \pm 0.7	7.2 \pm 0.9	3.72	
133	0.62115	6.5 \pm 1.8	6.3 \pm 1.3	6.4 \pm 1.1	4.49	
333	0.74040	5.6 \pm 1.0	---	5.6 \pm 1.0	4.58	
115	0.74040	4.9 \pm 0.5	---	4.9 \pm 0.5	4.58	
135	0.84292	5.1 \pm 0.8	---	5.1 \pm 0.8	4.63	
335	0.93433	3.0 \pm 1.5 (3.5 \pm 1.2 ^{**})	5.0 \pm 1.0	4.0 \pm 0.9	4.62	

* Employing data obtained from all the twelve observed reflections.

** Disregarding the intensities of the 533 and 335 reflections.

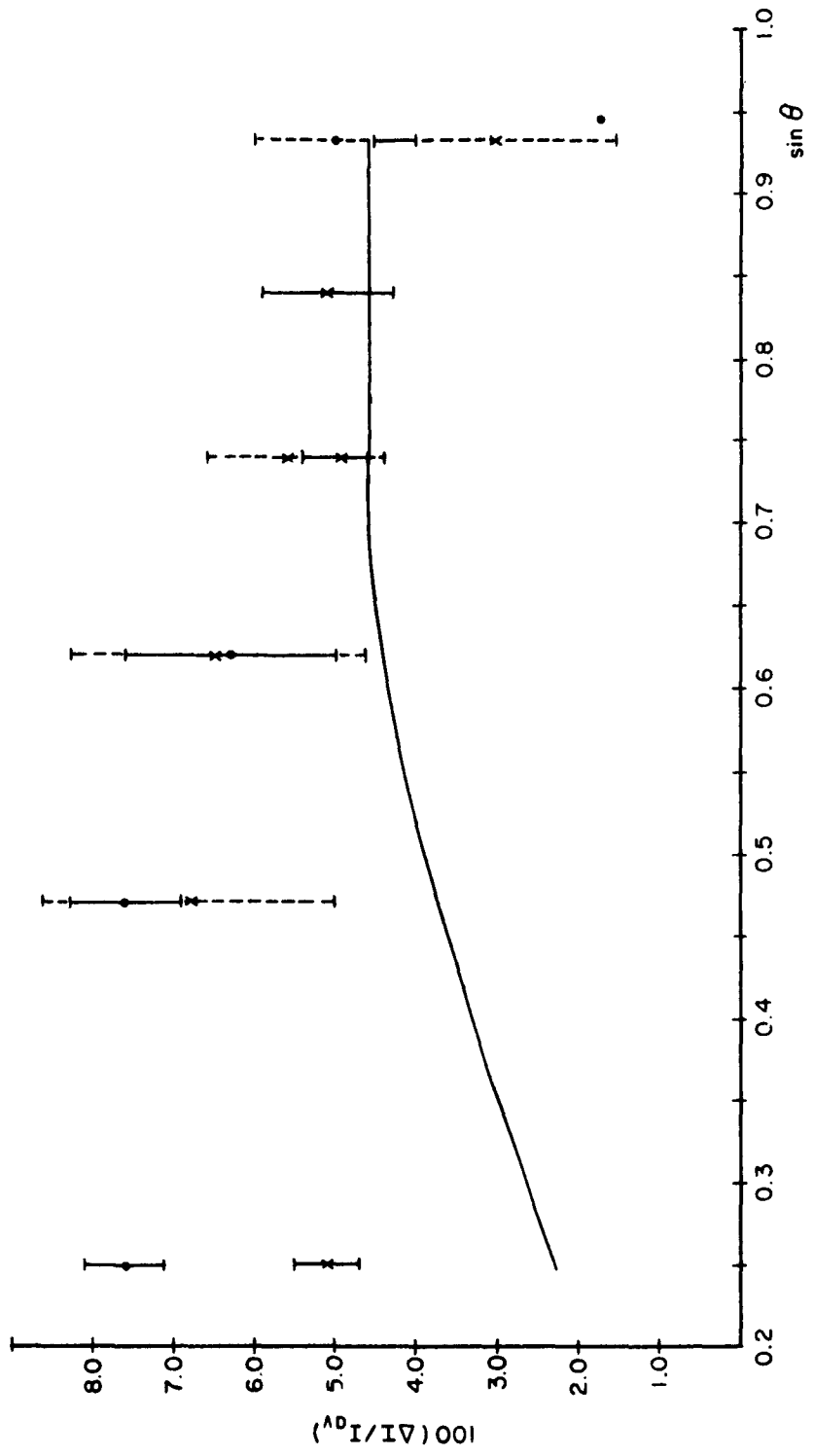


Fig. 3. $\Delta I/I_{av}$ as a function of $\sin \theta$ for ZnS with CuK α radiation.
x --- ZnS #1; • --- ZnS #2.

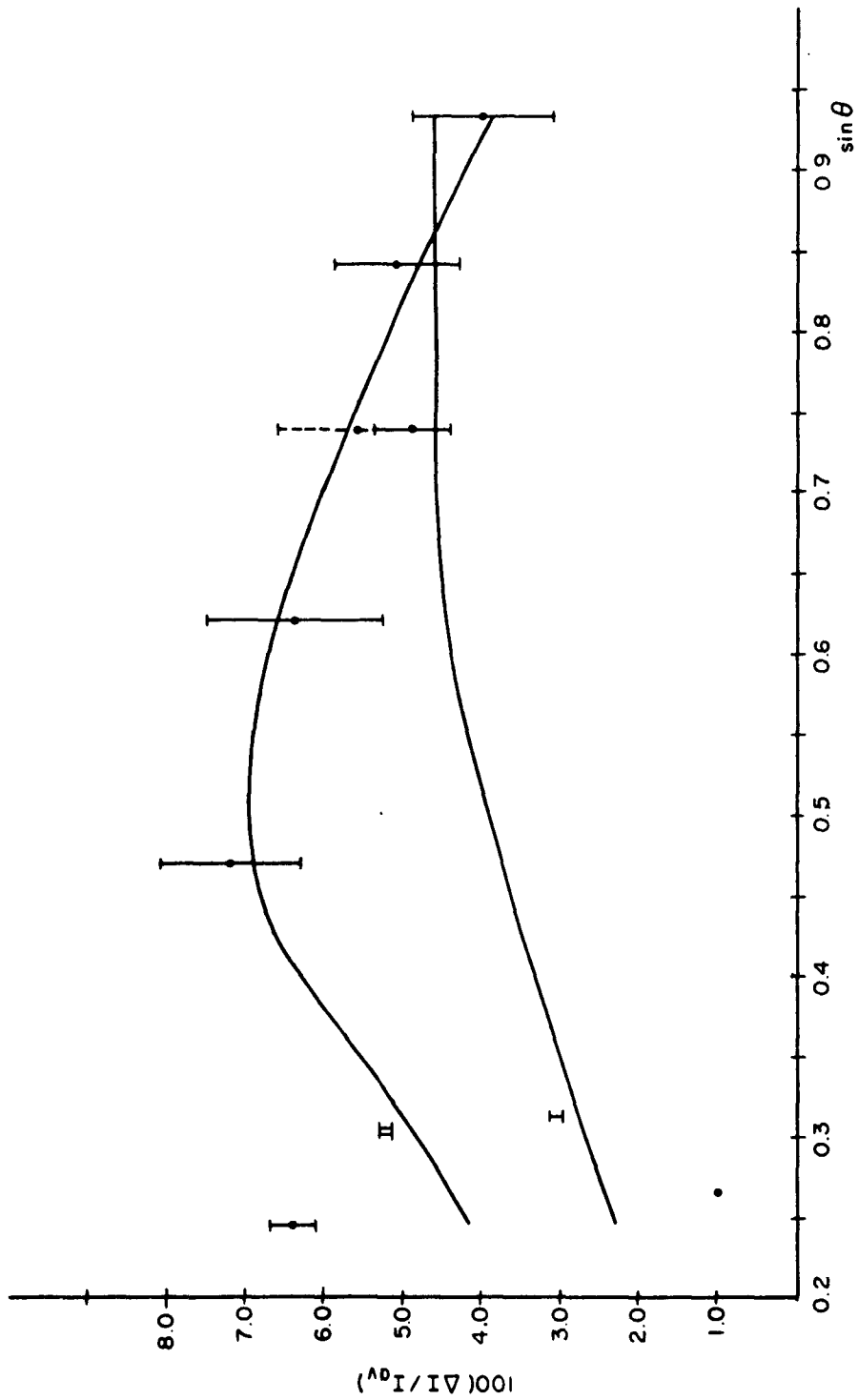


Fig. 4. Values of $\Delta I/I_{av}$ obtained by averaging the $\Delta I/I_{av}$ observed for ZnS #1 and ZnS #2 as a function of $\sin \theta$. The (333), (511), and (531) reflections were measured only for ZnS #1. Curve I -- theoretically predicted values of $\Delta I/I_{av}$ according to Templeton (11).

Curve II -- $\Delta I/I_{av}$ calculated assuming $\Delta f'_S = 1.85$ and $\Delta f''_{Zn} = 2.78$.

THE ANOMALOUS SCATTERING OF CHROMIUM $K\alpha$ RADIATION BY CUBIC ZINC SULFIDE

The intensities of three sets of reflections (six reflections in each set) with hkl odd were measured with chromium $K\alpha$ radiation. The diffracted radiation was filtered with a vanadium filter which transmitted 55 percent of the incident $K\alpha$ radiation. Pulse-height discrimination was employed to decrease the contribution to the intensity due to the white radiation, and the pulses from the proportional counter were amplified by a linear amplifier. The integrated intensities were obtained by scanning through an angular range of $3\frac{1}{3}^\circ$ 2θ at a rate of 1° 2θ per minute, and subtracting the background from the number of counts recorded by the scaler. The background was measured on both side of the peaks by noting the number of counts accumulated in the course of 200 seconds. All measurements were repeated at least three times.

Table 8 lists the experimental and theoretical values of $\Delta I/I_{av}$.

The agreement between equivalent reflections measured with $CrK\alpha$ radiation was poorer than with other radiations. This was ascribed to the high absorption coefficient of zinc sulfide for the soft chromium radiation, which tended to accentuate slight changes in the diameter of the spherical crystal. Results which have been discarded in the calculation of the experimental values of $\Delta I/I_{av}$ have been marked in Table 7 by an asterisk.

Table 7. Intensities of reflections with hkl odd for ZnS #1 (CrK α radiation).

hkl	Counts	a.d.	hkl	Counts	a.d.
1 $\bar{1}$ 1	41425	744	$\bar{1}$ $\bar{1}$ 3	48820	235
11 $\bar{1}$	39450		3 $\bar{1}$ $\bar{1}$	44180*	
$\bar{1}$ 11	40053		$\bar{1}$ 3 $\bar{1}$	49290	
$\bar{1}$ $\bar{1}$ 1	42253	710	13 $\bar{3}$	138750	1761
$\bar{1}$ 1 $\bar{1}$	43672		$\bar{3}$ 13	142271	
1 $\bar{1}$ $\bar{1}$	36857*		3 $\bar{3}$ 1	132730*	
$\bar{3}$ 11	54322*		$\bar{1}$ $\bar{3}$ 3	154605	785
1 $\bar{3}$ 1	52761	15	3 $\bar{1}$ $\bar{3}$	149630*	
11 $\bar{3}$	52792		$\bar{3}$ 3 $\bar{1}$	153035	

Table 8. Experimental and theoretical values of $\Delta I/I_{av}$ for zinc sulfide (CrK α radiation).

hkl	$\sin \theta$	$100(\Delta I/I_{av})_{obs}$	Theoretical values Dauben and Templeton
111	0.36658	6.4 ± 2.5	5.17
113	0.70103	7.3 ± 0.5	7.71
133	0.92321	9.0 ± 1.3	9.45

* Results which have been discarded in the calculation of $\Delta I/I_{av}$.

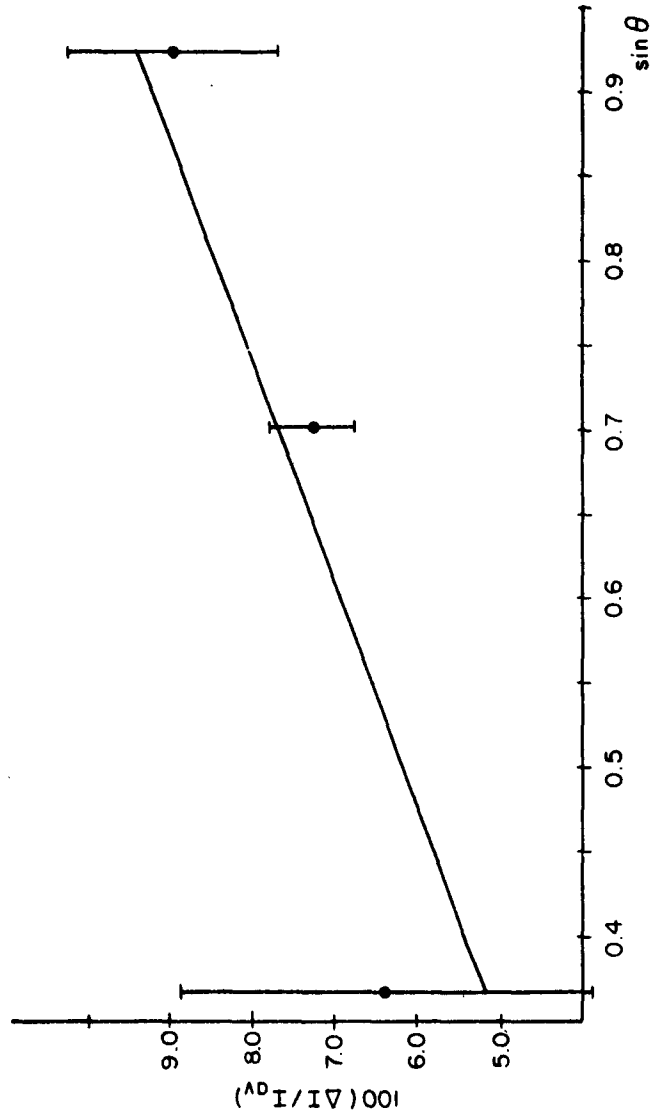


Fig. 5. $\Delta I/I_{av}$ as a function of $\sin \theta$ for ZnS with CrK α radiation. ● --- experimental values. Solid curve -- theoretical values calculated by using the dispersion corrections from the International Tables (11).

THE ANOMALOUS SCATTERING OF COPPER AND CHROMIUM K_{α} RADIATION
BY BORON PHOSPHIDE

The boron phosphide crystals were obtained from the Research and Engineering Division of Monsanto Chemical Company.* The translucent reddish crystals were reported to contain about 10^{18} impurities per cubic centimeter (24).

Considerable difficulties were encountered in grinding the crystals to spherical shape. A conventional emery-paper lined grinder produced no results. The diamond-dust lined grinder yielded imperfect spheres which exhibited deep pits. On further grinding these spheres turned into dust which escaped from the grinder. Investigation of the pitted spheres showed that they were mostly not single. By careful adjustment of the rate of flow of air through the grinder and by shortening the period between inspections of the grinder to 50 seconds, it became possible to observe (with the aid of a binocular microscope) the debris of a pitted sphere. These were found to contain several spheres about 0.1 mm in diameter. One of these, 0.105 ± 0.002 mm in diameter, was mounted with shellac on the sharp tip of a soft-glass fiber, similar to that used for zinc sulfide.

The difficulties encountered in grinding the spheres must be attributed to the smallness of the single crystals which constituted the initial crystal before grinding began.

*I would like to take this opportunity to thank Dr. Forrest V. Williams and Dr. B.D. Stone for providing the boron phosphide crystals prepared in their laboratory.

Possibly the crystal was further shattered in the process of grinding.

Rotation photographs showed the boron phosphide sphere to be single; no strain was apparent.

The measurements of the intensities of all reflections accessible to copper K α radiation were conducted following the same procedure as for zinc sulfide (ZnS #2).

The intensities of two sets of reflections were also measured with vanadium-filtered chromium radiation. The measurement procedure followed was the same as in the case of ZnS #1 and chromium radiation.

The theoretical values of $\Delta I/I_{av}$ in Tables 10 and 12 were calculated using the atomic scattering factors found in the International Tables (11). The real and imaginary dispersion corrections of boron were assumed to be zero. The dispersion corrections for phosphorus used in the two sets of values were found in the International Tables (11) and interpolated from James' tables (8), respectively.

ATTEMPT TO EVALUATE THE REAL AND IMAGINARY CORRECTIONS TO THE
 ATOMIC SCATTERING FACTORS OF PHOSPHORUS FROM THE EXPERIMENTAL
 RESULTS

The absence of real and imaginary corrections to the atomic scattering factors of boron leads to the following simplifications in the structure factors of boron phosphides:

$$|F|^2 = 16[f_B^2 + 2f_B f_p' + f_p'^2 + \Delta f_p''^2] \quad \text{when } h+k+l = 4n \quad (22)$$

$$|F|^2 = 16[f_B^2 - 2f_B f_p' + f_p'^2 + \Delta f_p''^2] \quad \text{when } h+k+l = 2n \quad (23)$$

$$|F|^2 = 16[f_B^2 - 2f_B \Delta f_p'' + f_p'^2 + \Delta f_p''^2] \quad \text{when } h+k+l = 4n+1 \quad (24)$$

$$|F|^2 = 16[f_B^2 + 2f_B \Delta f_p'' + f_p'^2 + \Delta f_p''^2] \quad \text{when } h+k+l = 4n-1, \quad (25)$$

where f_p' is the real part of the atomic scattering factor of phosphorus corrected for dispersion, $\Delta f_p''$ is its imaginary correction, and f_B is the atomic scattering factor of boron.

Subtracting (23) from (22) and (25) from (24), we obtain

$$D_1 = 64f_B f_p' \quad (26)$$

$$D_2 = -64f_B \Delta f_p'' \quad (27)$$

where D_1 and D_2 are intensity differences obtained by interpolating the experimental results.

Division of (27) by (26) yields

$$D_2/D_1 = -\Delta f_p''/(f_p' + \Delta f_p''). \quad (28)$$

Expression (28) is seen to give a set of linear simultaneous equations which can be solved by the least-square method.

Unlike $\Delta I/I_{av}$, (28) is independent of temperature effects at all Bragg angles.

Unfortunately, the attempt to utilize this method with the data obtained for boron phosphide failed. This must be ascribed mainly to the paucity of the data accessible to $\text{CuK}\alpha$ radiation, and partly to the insufficient precision of the obtained data.

Table 9. Integrated intensities of boron phosphide (CuK α radiation).

hkl	Counts	a.d.	hkl	Counts	a.d.
1 $\bar{1}$ 1	324577	1454	0 $\bar{4}$ 0	107930	
11 $\bar{1}$	321953		00 $\bar{4}$	106953	
$\bar{1}$ 11	320657		$\bar{4}$ 00	114277	
1 $\bar{1}$ $\bar{1}$	326090*		1 $\bar{3}$ 3	87467	457
$\bar{1}$ 1 $\bar{1}$	300363	3689	31 $\bar{3}$	86777	
$\bar{1}$ $\bar{1}$ 1	307740		$\bar{3}$ 31	86100	
0 $\bar{2}$ 0	173853		3 $\bar{3}$ $\bar{1}$	83563	360
00 $\bar{2}$	170237		$\bar{1}$ 3 $\bar{3}$	82810	
$\bar{2}$ 00	187907		$\bar{3}$ $\bar{1}$ 3	82696	
2 $\bar{2}$ 0	192773		4 $\bar{2}$ 0	55553	
$\bar{2}$ 20	191526		04 $\bar{2}$	55390	
$\bar{1}$ 3 $\bar{1}$	118457	910	$\bar{2}$ 4 $\bar{2}$	127900	
$\bar{1}$ $\bar{1}$ 3	118356		4 $\bar{2}$ $\bar{2}$	128410	
3 $\bar{1}$ $\bar{1}$	116733		3 $\bar{3}$ $\bar{3}$	120632	558
$\bar{3}$ 11	113967	1295	$\bar{3}$ 3 $\bar{3}$	121230	
1 $\bar{3}$ 1	111819		$\bar{3}$ $\bar{3}$ 3	122186	
11 $\bar{3}$	115500		3 $\bar{3}$ 3	115693	1252
2 $\bar{2}$ 2	74311		33 $\bar{3}$	113524	
22 $\bar{2}$	72283		$\bar{3}$ 33	112226	
$\bar{2}$ 22	72498		1 $\bar{5}$ 1	123630	349
$\bar{2}$ $\bar{2}$ 2	72880		11 $\bar{5}$	124180	
2 $\bar{2}$ $\bar{2}$	74027		$\bar{5}$ 11	124650	
$\bar{2}$ 2 $\bar{2}$	71747				

Table 9 (continued)

hkl	Counts	a.d.	hkl	Counts	a.d.
5 $\bar{1}\bar{1}$	116503	932	0 $\bar{4}$ 4	276336	
1 $\bar{5}\bar{1}$	116127		04 $\bar{4}$	275588	
1 $\bar{1}$ 5	118413				

Table 10. Experimental and theoretical values of $\Delta I/I_{av}$ for boron phosphide (CuK α radiation).

hkl	sin θ	100($\Delta I/I_{av}$) _{obs}	Theoretical values	
			Dauben and Templeton	Hönl
111	0.29387	5.7 \pm 1.3 (3.5) [*]	4.56	3.43
113	0.56309	3.5 \pm 1.2	5.17	3.87
133	0.73975	4.4 \pm 0.7	6.00	4.49
333	0.88188	6.4 \pm 1.2	7.07	5.26
115	0.88188	5.9 \pm 0.8	7.07	5.26

^{*}Using the data from all six 111 reflections.

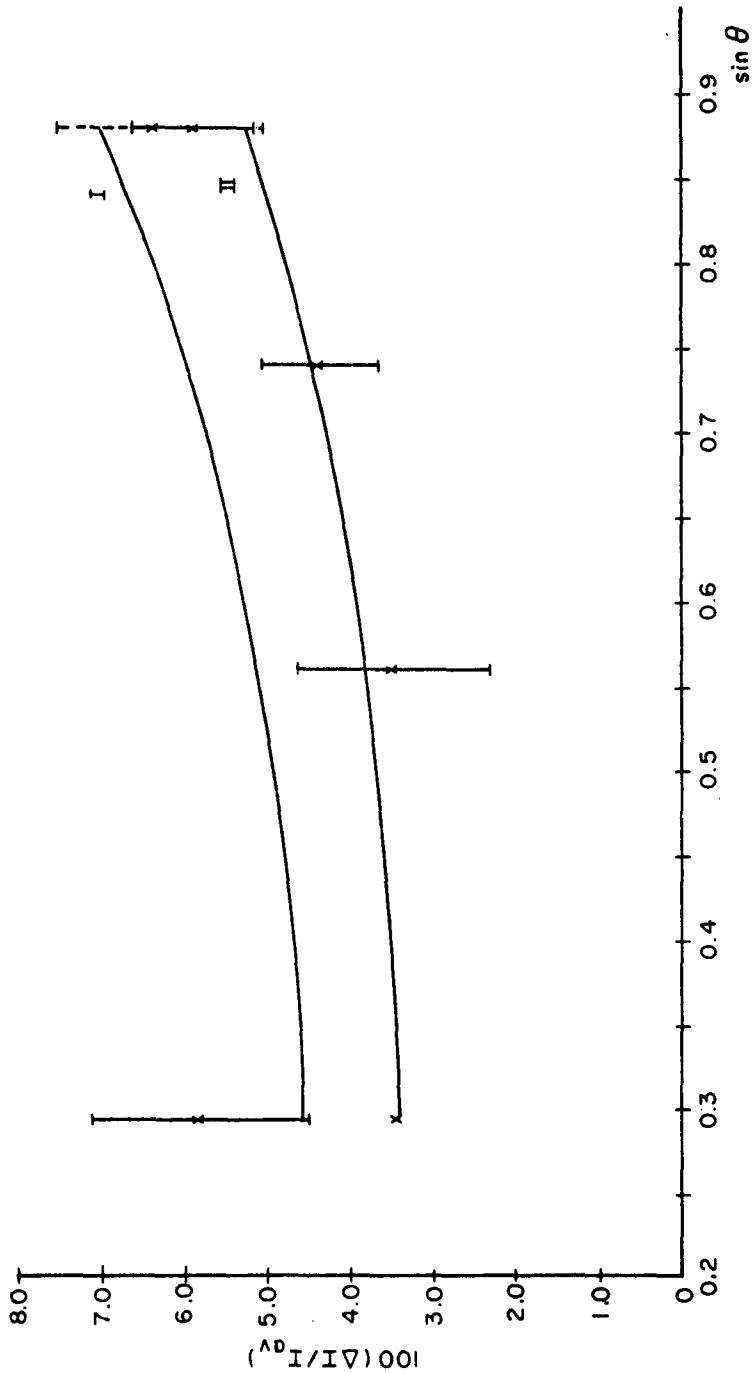


Fig. 6. $\Delta I/I_{av}$ as a function of $\sin \theta$ for BP (CuK α radiation). Curve I -- theoretical values calculated using the dispersion corrections listed in the International Tables. Curve II -- theoretical values obtained by using the dispersion corrections calculated from Hönl's work. The lower experimental value of $\Delta I/I_{av}$ at $\sin \theta \approx 0.294$ is obtained when no (111) intensities are discarded (cf. Table 10).

Table 11. Integrated intensities of boron phosphide (CrK α radiation).

hkl	Counts	a.d.	hkl	Counts	a.d.
11 $\bar{1}$	91902	257	11 $\bar{3}$	78935	209
1 $\bar{1}$ 1	96232*		1 $\bar{3}$ 1	78913	
$\bar{1}$ 11	92928		$\bar{3}$ 11	79395	
$\bar{1}$ 1 $\bar{1}$	87210	300	$\bar{1}$ 3 $\bar{1}$	85327	368
$\bar{1}$ $\bar{1}$ 1	87157		$\bar{1}$ $\bar{1}$ 3	84662	
1 $\bar{1}$ $\bar{1}$	87859		3 $\bar{1}$ $\bar{1}$	84338	

Table 12. Experimental and theoretical values of $\Delta I/I_{av}$ for boron phosphide (CrK α radiation).

hkl	sin θ	100($\Delta I/I_{av}$) _{obs}	Theoretical values	
			Dauben and Templeton	Hönl
111	0.43680	5.6 \pm 0.4	8.38	7.63
113	0.83686	7.0 \pm 0.5	9.01	8.55

*Discarded in calculating ($\Delta I/I_{av}$)_{obs}.

DISCUSSION OF EXPERIMENTAL RESULTS

The results obtained for ZnS with MoK α radiation are in general but not complete agreement with the theoretical values, being slightly lower than the theoretical values of $\Delta I/I_{av}$ in the range of low Bragg angles and higher at high Bragg angles (Fig. 2). A change in the temperature factors which would improve agreement at higher Bragg angles would increase the discrepancy at lower θ by a negligible amount. This indicates a need for revision of the imaginary corrections of zinc and sulfur for MoK α radiation. A calculation of these corrections from low- θ reflections (along the same lines as was done for the case of CuK α radiation) may yield experimental values of $\Delta f''$ which may in turn be applied to the reflections occurring at intermediate θ to obtain temperature factors. It has been noted that the spread of the experimental values from a smooth curve of $\Delta I/I_{av}$ vs $\sin\theta$ exceeds the estimated experimental errors; this may in part be due to the effectively anisotropic nature of the temperature factors, such as would result from anharmonic contributions to the temperature motion. The fact that the dispersion corrections due to Hönl and those due to Templeton for zinc and sulfur are almost equal at the MoK α wavelength makes it difficult in this case to decide about the relative merits of the two approaches.

The large discrepancy between the experimentally obtained values of $\Delta f''$ for zinc and sulfur with CuK α radiation and the theoretical values is probably caused by the extreme

proximity of the K absorption edge of zinc ($\lambda = 1.283 \overset{\circ}{\text{A}}$). In cases such as this experimental data are essential.

The data obtained for zinc sulfide with $\text{CrK}\alpha$ radiation agree within experimental error with the values of $\Delta I/I_{\text{av}}$ calculated with Templeton's dispersion corrections, and this is not surprising considering the fact that this wavelength is quite far from any absorption edge.

The agreement between the experimental results obtained for boron phosphide with $\text{CuK}\alpha$ radiation and those calculated using Hönl's corrections is good except in the case of the (111) reflections where errors due to absorption affect the results considerably. The values obtained for the (333) and (115) reflections are somewhat too high and would agree better with Hönl's corrections if temperature effects were allowed for. The case of boron phosphide with $\text{CuK}\alpha$ radiation is of particular interest, since it appears to indicate that Hönl's, rather than Templeton's, corrections should be preferred, at least in this case. It must, of course be kept in mind that Hönl's corrections are approximate, taking account only of dispersion effects due to the K electrons. However, in the case of phosphorus Hönl's corrections will most probably remain unaffected by the other electrons (the L absorption edge is between 76 and 127 $\overset{\circ}{\text{A}}$).

In conclusion it should be noted that a choice between the approaches of Dauben and Templeton and Hönl can best be made at wavelengths where their results differ considerably, and possibly with relatively light elements where effects due

to other electron shells are negligible. To facilitate the comparison between the results of Dauben and Templeton and Hönl, a table of Hönl's corrections for commonly used wavelengths is indispensable. Values for such a table are being calculated with the aid of an electronic computer.

An extension of the calculations of Eisenlohr and Müller to include effects due to the L electrons to a number of elements (Zn, S, P, etc) would also be of considerable interest.

APPENDIX

THE BALANCING OF FILTERS FOR COPPER K_{α} RADIATION

The well-known method of balanced filters, devised by Ross (28) and developed by Kirkpatrick (29) and others, was employed to exclude wavelengths emitted by the copper target which fall outside the passband between 1.4880 and 1.6081 \AA (the K absorption edges of nickel and cobalt).

In spite of the additional time required to collect the data and the comparatively wide passband, the use of balanced filters offers some advantages over crystal monochromators which yield relatively weak, partly polarized beams, deteriorate upon prolonged exposure to x rays in a humid atmosphere, and whose use makes it difficult to exclude unwanted wavelengths due to higher-order reflections.

The following procedure was employed to obtain the required balance of the filters. A strong reflection was brought into diffracting position and the output of the copper tube from the short-wavelength cutoff to the long-wavelength side of the K_{α} peak was recorded. The same range was then scanned with a filter made of finely powdered cobalt oxide suspended in a plastic binding material. The height of the maximum of the K_{β} peak was carefully noted and the cobalt-oxide filter was replaced by a 0.00053-cm nickel foil. The nickel foil was tilted until the K_{β} peak became equal to that previously observed with the cobalt oxide. A repetition of the scan over the same range as with the cobalt-oxide filter indicated that the filters were now almost

balanced at all wavelengths, except at the long-wavelength side of the $K\alpha$ peak where the nickel filter transmitted slightly more radiation. After trying several substances, it was found that when 0.001 cm aluminum foil is added to the nickel foil and both are tilted at about 65° to the diffracted beam the balance obtained at all wavelengths is very good. Figure 7 in which the two scans with the balanced filters are superimposed illustrates the final results. The nickel-and-aluminum filter transmitted 60.4 percent of the incident $K\alpha$ radiation.

The nickel and aluminum foils were mounted in a specially designed holder* which allowed the foils to be tilted relative to the diffracted beam. The design of the holder allowed firm locking of the filters in their tilted position. The insertion and removal of the holder were easy and reproducible.

It should be noted that while pulse-height discrimination will not destroy the balance, it will also not improve it. The sole advantage of pulse-height discrimination used in conjunction with balanced filters is to diminish the relative weight of balancing errors (cf. reference 30).

* It is my pleasant duty to thank Mr. K. Hale and Mr. J. Shapiro for constructing the holder in the instrument shop of the Physics Department of the Polytechnic Institute of Brooklyn.

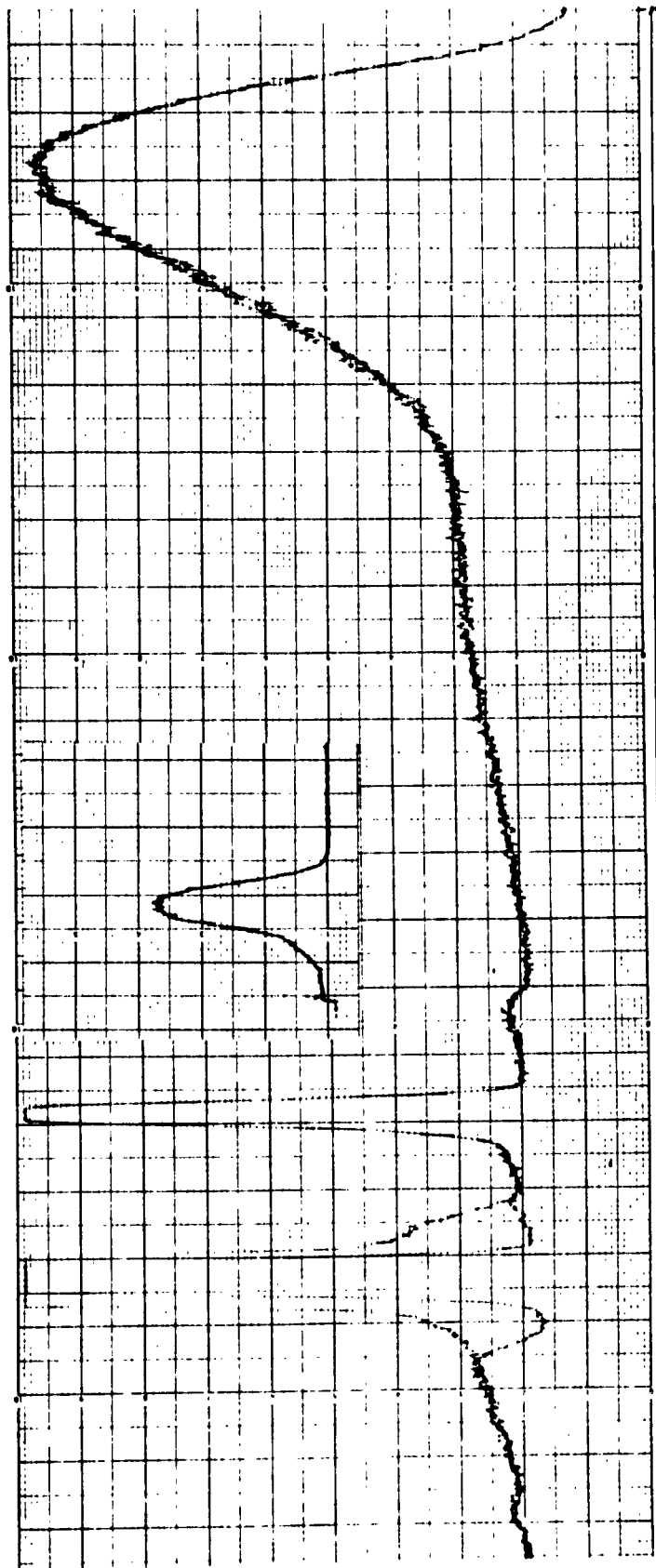


Fig. 7. Superimposed emission spectra of copper taken with balanced nickel and cobalt filters. Insert -- $K\beta$ on a higher scale factor.

BIBLIOGRAPHY

1. H. Hönl, Z. Physik 84, 1 (1933).
2. L.G. Parratt and C.F. Hempstead, Phys. Rev. 94, 1593 (1954).
3. Townsend, Jeffrey, and Panagis, Z. für Kristallographie 112, 150 (1959).
4. J. Friedman, Thesis, Polytechnic Institute of Brooklyn, 1960.
5. A.H. Compton and S.K. Allison, X-Rays in Theory and Experiment, (Van Nostrand Co., 1954).
6. R. Glocker and K. Schäfer, Z. Physik 73, 289 (1931).
7. Y. Sugiura, J. de Physique 8, 113 (1928).
8. R.W. James, The Optical Principles of the Diffraction of X-Rays, (Bell and Sons Ltd., London, 1958).
9. H. Eisenlohr and G.L.J. Müller, Z. Physik 136, 491, 511 (1954).
10. C.H. Dauben and D. H. Templeton, Acta Cryst. 8, 841 (1955).
11. International Tables for X-Ray Crystallography, (The Kynoch Press, Birmingham, 1962) Vol. III.
12. H. Mark and L. Szilard, Z. Physik 33, 688 (1925).
13. A.H. Armstrong, Phys. Rev. 34, 931 (1929).
14. R.W.G. Wyckoff, Phys. Rev. 35, 583 (1930), and *ibid.* 36, 1116 (1930).
15. A.J. Bradley and R.A.H. Hope, Proc. Roy. Soc. A136, 272 (1932).
16. A. Rusterholz, Z. Physik 82, 538 (1933).
17. G.W. Brindley and F.W. Spiers, Phil. Mag. 20, 865 (1935).
18. J.C.M. Brentano and A. Baxter, Z. Physik 89, 720 (1934).
19. S. Nishikawa and K. Matukawa, Proc. Imp. Acad. Tokyo 4, 96 (1928).

20. Coster, Knol, and Prins, Z. Physik 63, 345 (1930).
21. Harrison, Jeffrey, and Townsend, Acta Cryst. 11, 552 (1958).
22. Dana's System of Mineralogy, C. Palache, H. Berman, and C. Frondel (Wiley and Sons Inc., London, 1944) Vol. I.
23. D.P. Miller, Thesis, Polytechnic Institute of Brooklyn, 1962.
24. F.V. Williams, private communication.
25. J.M. Bijvoet, Nature 173, 888 (1954).
26. R.B. Roof, Jr., Acta Cryst. 14, 934 (1961).
27. Perri, LaPlaca, and Post, Acta Cryst. 11, 310 (1958).
28. P.A. Ross, Phys. Rev. 28, 425 (1926).
29. P. Kirkpatrick, Rev. Sci. Instr. 27, 12 (1939).
30. Soules, Gordon, and Shaw, Rev. Sci. Instr. 27, 12 (1956).

INVESTIGATION OF THE ENERGY LEVELS OF MAGNETIC IONS
IN THE COMPLEX METAL OXIDES, ESPECIALLY IN THE ORTHOFERRITES

DISTRIBUTION LIST

<u>Code</u>	<u>Organization</u>	<u>No. of Copies</u>
AF 5	AFMTC (AFMTC Tech. Library-MU-135) Patrick AFB, Florida.	1
AF 18	AUL Maxwell AFB, Alabama.	1
AF 32	OAR (RROS, Col. John R. Fowler) Tempo D 4th and Independence Ave., Washington 25, D.C.	1
AF 33	AFOSR, OAR (SRYP) Tempo D 4th and Independence Ave., Washington 25, D.C.	1
AF 43	ASD (ASAPRD - Dist) Wright-Patterson AFB, Ohio	1
AF 124	RADC (RAALD) Griffiss AFB, New York Attn: Documents Library	1
AF 139	AF Missile Development Center (MDGRT) Holloman AFB, New Mexico	1
AF 314	Hq. OAR (RROSP, Maj. Richard W. Nelson) Washington 25, D.C.	1
Ar 5	Commanding General USASRDL Ft. Monmouth, N.J. Attn: Tech. Doc. Ctr. SIGRA/SL-ADT	1
Ar 9	Department of the Army Office of the Chief Signal Officer Washington 25, D.C. Attn: SIGRD-4a-2	1
Ar 50	Commanding Officer Attn: ORDTL-012 Diamond Ordnance Fuze Laboratories Washington 25, D.C.	1

Ar 67	Redstone Scientific Information Center U.S. Army Missile Command Redstone Arsenal, Alabama	1
G 31	Office of Scientific Intelligence Central Intelligence Agency 2430 E Street, N.W. Washington 25, D.C.	1
G 2	ASTIA (TIPAA) Arlington Hall Station Arlington 12, Virginia	10
G 68	Scientific and Technical Information Facility Attn: NASA Representative (S-AK-DL) P.O. Box 5700 Bethesda, Maryland	1
G 109	Director Langley Research Center National Aeronautics and Space Administration Langley Field, Virginia	1
N 9	Chief, Bureau of Naval Weapons Department of the Navy Washington 25, D.C. Attn: DLI-31	2
N 29	Director (Code 2027) U.S. Naval Research Laboratory Washington 25, D.C.	2
I 292	Director, USAF Project RAND The Rand Corporation 1700 Main Street Santa Monica, California Thru: AF Liaison Office	1
M 6	AFCRL, OAR (CRXRA - Stop 39) L.G. Hanscom Field Bedford, Mass.	20
AF 253	Technical Information Office European Office, Aerospace Research Shell Building, 47 Cantersteen Brussels, Belgium	1
AR 107	U.S. Army Aviation Human Research Unit U.S. Continental Army Command P. O. Box 428, Fort Rucker, Alabama Attn: Maj. Arne H. Eliasson	1

G 8	Library Boulder Laboratories National Bureau of Standards Boulder, Colorado	2
M 63	Institute of the Aerospace Sciences, Inc. 2 East 64th Street New York 21, New York Attn: Librarian	1
M 84	AFCRL, OAR (CRXR, J. R. Marple) L. G. Hanscom Field Bedford, Massachusetts	1
N 73	Office of Naval Research Branch Office, London Navy 100, Box 39 F.P.O., New York, New York	5
U 32	Massachusetts Institute of Technology Research Laboratory Building 26, Room 327 Cambridge 39, Massachusetts Attn: John H. Hewitt	1
U 431	Alderman Library University of Virginia Charlottesville, Virginia	1
G 9	Defense Research Member Canadian Joint Staff 2450 Massachusetts Avenue, N.W. Washington 8, D.C.	1
AF 318	Aero Res. Lab. (OAR) AROL Lib. AFL 2292, Bldg. 450 Wright-Patterson AFB, Ohio	1
AF 3	Aeronautical Research Laboratories, OAR (ARX) Attn: Mr. Marshall Kreitman Solid State Physics Research Laboratory Wright-Patterson AFB, Ohio	1
	Hq. AFCRL, OAR (CRR CSP-3, Peter D. Gianino) L. G. Hanscom Field Bedford, Massachusetts	9